TECHNICAL ARTICLE

Evaluation of Thermal Comfort Inside an Office Equipped with a Fan Coil HVAC System: A CFD Approach

Giovanni Semprini, Aminhossein Jahanbin, Beatrice Pulvirenti and Paolo Guidorzi

An accurate assessment of thermal comfort inside a building is essential since it is associated to the human's perception of well-being and comfort. In the present study, a 3D computational fluid dynamic (CFD) code is employed to evaluate the indoor comfort indexes for a university office located in a historical building, built of thick masonry walls and of large single-glass windows, using fan coil as an air conditioning system. The experimental measurement has been carried out to validate the numerical model and to obtain the required initial and boundary conditions. The experimental set-up employs an innovative system for the sensor localization, based on acoustic sources, signal processing and trilateration algorithms. By means of finite volume method, the turbulent air flow, the local heat transfer characteristics and the operative temperature inside the room are obtained for a typical winter day. The results yielded by numerical simulations allow to evaluate thermal comfort condition at working places inside the office and to identify the best comfort areas. The results show that even when the air temperature is quite uniform inside the room, the operative temperature at the positions where occupants are placed is significantly affected by surface temperature of the windows, due to the large window to wall surface ratio and also by the position and operational condition of fan coil. It is concluded that 3D comfort map allows to optimize internal layout of the office room; furthermore, the possibility of thermal comfort optimization in specific workstation together with local control of heating system lead to gain remarkable energy saving results.

Keywords: thermal comfort; operative temperature; CFD simulation; HVAC system; energy efficiency

1. Introduction

Most industrialized countries, in particular the European Union countries, are in shifting phase from a fossil-based development to a sustainable development. Approximately 40% of the energy consumption in the European Union is attributed to buildings across the private and public sectors. The European Parliament Directive 2010/31 (The Directive 2010/31/EU) states that new buildings should consume very low amount of fossil-based energy (Nearly Zero Energy Buildings) by 2020. The Directive declares that all new buildings built after 31 December 2018 will have to be buildings with high energy performance and their required amount of energy should be mostly covered by renewable energy sources. Hence, energy efficiency has become a common target for all buildings, in particular historical buildings (Fotopoulou et al. 2018). Since buildings with historic value are less energy-efficient than modern ones, energy demand and indoor comfort expectations are critical challenges for them.

Indeed, indoor thermal comfort in a moderate environment is considered as the human's perception of well-being and satisfaction. Thermal comfort is defined by ASHRAE (2013) as "that condition of mind that express satisfaction with thermal environment and is assessed by subjective evaluation". Overall thermal comfort and the assessment of indoor environment quality depend not only on physical parameters but also on psychological and physiological response of the human's body to the environment. Thermal comfort can be evaluated by either classic approach introduced by Fanger (1970) or adaptive approach (Nicol et al. 2015). The classic approach interprets the global and local thermal comfort by means of two indexes: Predicted Mean Vote (PMV) and Predicted Percentage of Dissatisfied (PPD), adopted also in ISO 7730 (2005). However, acquisition of the required data to predict thermal comfort is not an easy task; it is time demanding and requires specific instruments to calculate the relevant parameters.

An interesting alternative technique to predict thermal comfort could be simulations implemented by Computational Fluid Dynamic (CFD) codes, allowing to analyse thermo-hydraulic characteristics within environments. Several studies were conducted in order to determine the thermal comfort with CFD simulations in

Department of Industrial Engineering, University of Bologna, Bologna, IT

Corresponding author: Giovanni Semprini (giovanni.semprini@unibo.it)

various environments such as office room (Stamou and Katsiris 2006), educational building (Buratti et al. 2017), theatre (Cheong et al. 2003), stadium (Stamou et al. 2008), museum (Papakonstantinou et al. 2000) and test room (Catalina et al. 2009). For instance, Sevilgen and Kilic (2011), by means of finite volume method, performed a 3D steady-state analysis of a room heated by two-panel radiators. A virtual sitting manikin with real dimensions and physiological shape was added to the model of the room, and two different pairs of heat transfer coefficients of outer wall and window were considered. The obtained results showed that better-insulated wall and window could enhance thermal comfort while reducing the energy consumption.

A 3D numerical model was employed by Nada et al. (2016) to investigate the airflow, temperature distribution and thermal comfort in a high-rise ceiling theatre air conditioned with UnderFloor Air Distribution (UFAD). The results showed that the numerical model can accurately predict the airflow and temperature distribution in the high-rise conditioned space and that the low air velocities of a UFAD provide the appropriate level of environmental comfort. It was recommended to use higher numbers of diffusers for achieving better thermal comfort condition.

Buratti et al. (2017) employed a CFD tool together with the experimental data to predict indoor condition and thermal comfort inside a room, by setting only external weather conditions as input parameters. The survey and data acquisition for evaluation of thermal comfort were carried out in a classroom at the department of engineering, university of Perugia. It was concluded that CFD code could be a very useful and cost-effective tool to support the experimental campaign and to evaluate the thermal local sensation.

Cheong et al. (2020) presented a simulation-aided approach for analysing and optimizing lighting and thermal conditions in building interior. A finite volume CFD code was adopted for prediction of air flow and ambient temperature. A methodology on a real-world case study on an office building in Singapore was demonstrated, improving lighting and thermal conditions greatly through passive daylight fixtures and the reconfiguration of climate-control air supply vents within the office space. The obtained results showed a significant reduction in energy consumption and enhancement of indoor environmental quality.

Thermal comfort in office rooms has been widely investigated both to increase people satisfaction and also to analyse solutions to reduce energy consumption (Stamou and Katsiris 2006, Putra 2017, Maykot et al. 2018). In many situations, the internal layout of HAVC terminal systems and workstations inside a single room are not properly investigated in the design phase, causing gradient in temperature and air velocity with different comfort conditions for occupants. Furthermore, in existing historical buildings with low thermal performance, asymmetry of radiant temperature occurs in winter period and too high air temperature is set inside the rooms (Semprini et al. 2016). CFD analysis is an important tool in design phase for determination of the internal layout, the operation mode of terminals (inlet temperature, air flow), and the

position of sensors for room control system (Shahzad et al. 2017, Awwad et al. 2017): the latter plays an important role to maintain internal temperature set-point.

Accuracy of the CFD results depends mainly on the adopted boundary conditions and convection model. In application of CFD analysis to real buildings and large rooms, where many conditions affect the thermo-hydraulic behaviour of the air flow, some assumptions must be made and a comparison and/or calibration in specified conditions is recommended (Hajdukiewicz et al. 2013, Shan et al. 2019).

In the present paper, local thermal comfort in a university office room equipped with fan coil heating system has been evaluated in typical winter conditions. The case study is an office room located inside a typical historical building, built with thick masonry walls and large single-glass windows with high thermal transmittance. Architectural constraints, often combined to economic difficulties in those public buildings, prevent the use of retrofit technical solutions (wall insulation, new performing windows, local control system, etc.), causing high energy consumption due to higher indoor air temperatures (sometimes set at 23–24°C) while at the same time maintains local discomfort at working positions.

The analysis has been performed by means of CFD simulations and the numerical model is validated by experimental results. A new methodology for sensors localization based on acoustic signals sampling and processing is presented for the experimental measurement and model validation. The spatial distribution of the air temperature and velocity are presented and values of the operative temperature for specific positions inside the room are analysed. The obtained results allow to evaluate thermal comfort condition at working places, to evidence discomfort zones that are related to the characteristics of the building and heating system under study, and to identify the best comfort areas inside the office for optimum internal layout.

2. Numerical Method

The schematic of the computational domain under consideration is illustrated in **Figure 1**. It is composed of a
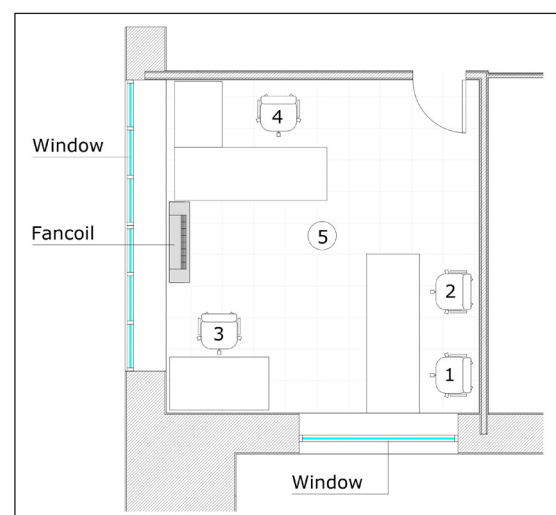

Figure 1: Schematic of the office under study.

4.73 m × 5.03 m office with 4.24 m height, equipped with a fan-coil air conditioning system, with an exit surface of the air of 0.08 m × 0.65 m = 0.052 m². The mean value of air velocity at the exit surface of the fan coil was measured equal to 0.8 m/s. The value of air temperature exiting from the fan coil, depending on the centralized water heating system, was measured in the range 33–34°C.

The office domain consists of two external walls with windows, and two internal walls. 5 specific positions inside the room was considered to evaluate the condition of thermal comfort: 4 working desks and the central point of the room. As boundary condition, the internal walls were assumed to be isothermal with measured mean value $T = 21°C$, while for the external walls boundary condition of third kind was considered, with convection coefficient $h = 25 \ W/m^2 k$. Surface walls of the floor and ceiling were considered as adiabatic, as they are adjoining to the heated room.

The thermophysical properties of moist air were calculated and employed in numerical simulations (Tsilingiris, 2008). The values of thermal properties of dry air at atmospheric pressure (Raznjevic, 1976) and of the saturation properties of water (Sontag, 2003) were adopted at reference temperature. The following values of the density, dynamic viscosity, specific heat capacity at constant pressure and thermal conductivity of moist air were obtained for $T = 20°C$: $\rho_m = 1.153 \ kg \ m^{-3}$, $\mu_m = 1.82 \times 10^{-5} \ kg \ m^{-1} \ s^{-1}$, $c_{pm} = 1020 \ J \ kg^{-1} \ K^{-1}$, and $k_m = 0.0253 \ W \ m^{-1} \ K^{-1}$. It should be noted that ρ_m is the reference value for the density of moist air. The fluid density term was considered to be constant except in the buoyancy force term, where it was assumed as a linear function of the temperature.

In analogy with recent literature on CFD simulations of the rooms equipped with a HVAC system (Sevilgen and kilic 2011, Maivel et al. 2015, Jahanbin and Zanchini 2016), a 3D steady-state thermo-hydraulic model was considered assuming the air flow inside the room turbulent. The governing equations, i.e. the mass, momentum and energy balance equations, can be written as:

$$\nabla \cdot \vec{v} = 0 \tag{1}$$

$$\rho_0 \left[\frac{\partial \vec{v}}{\partial t} + (\vec{v} \cdot \nabla)\vec{v} \right] = -\nabla(p + \rho_0 g z) + \rho_0 g \beta (T - T_0)\nabla z + \nabla \cdot \tilde{\tau}_{eff} \tag{2}$$

$$\frac{\partial}{\partial t}(\rho e) + \nabla \cdot (\vec{v}(\rho e + p)) = \nabla \cdot [(k + k_t)\nabla T + \tilde{\tau}_{eff} \cdot \vec{v}] \tag{3}$$

In Equations 1−3, $\vec{v}$ is the velocity vector, p is pressure, β is the thermal expansion coefficient, $\tilde{\tau}_{eff}$ is the effective stress tensor, $E = h - p/\rho + v^2/2$, h is specific enthalpy, v is the magnitude of $\vec{v}$, k is the thermal conductivity, k_t is the turbulent thermal conductivity and subscript 0 refers to the reference values. The effective stress tensor is given by:

$$\tilde{\tau}_{eff} = \tilde{\tau} + \tilde{\tau}_t \tag{4}$$

Among common turbulence models, the κ-ε model is the most widely used and validated model. It applies to a wide range of flows, which occur in many technical applications. The RNG (Renormalization Group) κ-ε model was selected for this study, due to the higher precision and stability rendering for internal flows (Choudhury 1993, Chen 1999). The RNG κ-ε model is quite similar to the classic κ-ε model but includes some refinements such as: enhanced accuracy for swirling flows, an analytically derived differential formula for effective-viscosity that accounts for low-Reynolds numbers effects, and an additional term in ε to improve accuracy. The RNG κ-ε model's governing equations are (Yakhot 1992, Versteeg 1995):

$$\frac{\partial(\rho\kappa)}{\partial t} + \nabla \cdot (\rho\kappa\vec{v}) = \nabla \cdot (\alpha_\kappa \mu_{eff} \nabla\kappa) + 2\mu_t E_{ij}E_{ij} - \rho\varepsilon \tag{5}$$

$$\frac{\partial(\rho\varepsilon)}{\partial t} + \nabla \cdot (\rho\varepsilon\vec{v}) = \nabla \cdot (\alpha_\varepsilon \mu_{eff} \nabla\varepsilon) + C_{1\varepsilon}^* \frac{\varepsilon}{\kappa} 2\mu_t E_{ij}E_{ij} - C_{2\varepsilon}\rho\frac{\varepsilon^2}{\kappa} \tag{6}$$

In Equations 5 and 6,

$$\mu_{eff} = \mu + \mu_t \ ; \quad \mu_t = \rho C_\mu \frac{\kappa^2}{\varepsilon} \tag{7}$$

where $C_\mu = 0.0845$. In addition, $\alpha_\kappa = \alpha_\varepsilon = 1.39$; $C_{1\varepsilon} = 1.42$; $C_{2\varepsilon} = 1.68$ and $C_{1\varepsilon}^* = C_{1\varepsilon} - \frac{\eta(1-\eta/\eta_0)}{1+\gamma\eta^3}$ where $\eta = \sqrt{2E_{ij}E_{ij}} \frac{\kappa}{\varepsilon}$ and $\eta_0 = 4.377$; $\gamma = 0.012$.

Radiation heat transfer was considered by applying the surface-to-surface radiation model (Siegel 1992). In this model, the air inside the room is considered as a transparent medium and all surfaces are assumed to be diffusive and grey. The following values were considered for the emissivity of surfaces: 0.88, 0.89, 0.87, and 0.9 for fan coil box, window (glass), door (glass), and walls, respectively (ASHRAE 2009).

The effects of solar loading are needed in many HVAC applications, where the temperature, humidity, and velocity fields around occupants are desired. In the present study, effect of solar irradiation on windows has been taken into account by means of the solar ray tracing algorithm, for different working hours namely at 9:00, 12:00, 15:00 and 18:00. The ray tracing approach is a highly efficient and practical means of applying solar loads as heat sources in the energy equations. The resulting heat flux is coupled to the calculation as a source term in the energy equation. The heat sources are added directly to computational cells bordering each face and are assigned to adjacent cells.

The values of direct solar irradiation and diffuse solar irradiation have been adopted from the data extracted from the Italia climatic data (De Giorgio), on February 6th for the Bologna, Italy, with latitude 44.4938°N and longitude 11.3387°E. **Figure 2** illustrates the variation of outdoor temperature, direct and diffuse solar irradiation during a typical winter day (February 6th) for Bologna, Italy. The values of direct solar irradiation are equal to 94.5, 325.7, 229 and 0 W/m² at 9:00, 12:00, 15:00 and 18:00 o'clock, respectively. Orientation of computational mesh with respect to the sun direction vector has been calculated by employing Solar Calculator program in the software. The values of spectral fraction and sunshine factor has been set equal to 0.5 and 0.65, respectively.

In order to calculate the operative temperature, T_{opr}, the equation recommended by ASHRAE (2013) was employed, namely:
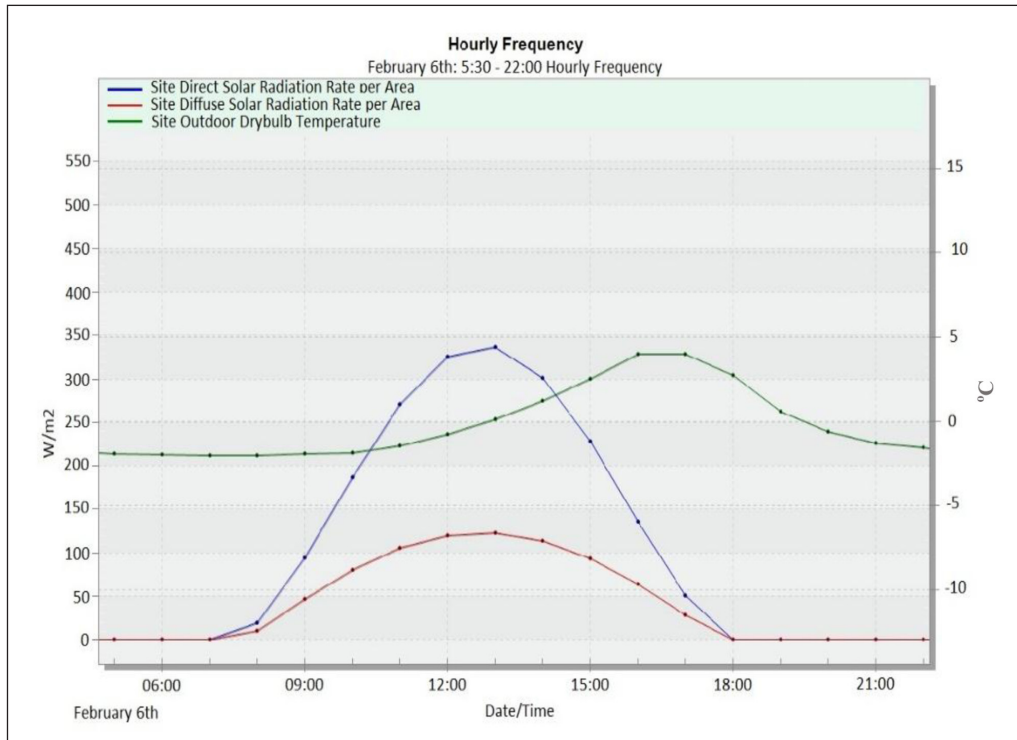
Figure 2: Outdoor temperature and solar irradiation (direct and diffuse) for a typical winter day of Bologna (Italia climatic data, De Giorgio).

$$T_{opr} = \psi T_{air} + (1 - \psi)T_{rad} \qquad (8)$$

where T_{air} is the air temperature, T_{rad} is the mean radiant temperature, and ψ is a weight factor depending on the air velocity; this factor is usually considered between 0.4 and 0.5. In this study, it was assumed equal to 0.5. The operative temperature is calculated inside the office for 5 different positions (at 4 working desks + central point of the room), as illustrated in **Figure 1**, for different working hours.

The mean radiant temperature of the room surfaces with respect to a virtual person inside the room is given by:

$$T_{rad} = \sum_{1}^{n} F_j T_{sj} \qquad (9)$$

where T_{sj} is the temperature of the j-th surface and F_j is the angular factor between the person and the j-th surface. In order to calculate view factors involved in Equation (9), a small cubic surface with size of 10 cm was considered as a local sensor at corresponding positions.

In general, thermal comfort is classified according to the type of environment: indoor, outdoor or semi-outdoor. In terms of indoor thermal comfort, the discussion centres mainly on two distinct approaches: classic steady-state model based on a heat balance model of human's body, developed by Fanger (1970), and adaptive model which is based on field studies in naturally ventilated buildings (Nicol et al. 2015). In the present study, Fanger's classic model has been employed to evaluate indoor thermal comfort condition. In fact, Fanger's model aims to predict mean thermal sensation of a group of people and their respective percentage of dissatisfaction with the thermal

environment, expressed through the indexes Predicted Mean Vote (PMV) and Predicted Percentage Dissatisfied (PPD) (Rupp et al. 2015). According to ASHRAE (2013) and ISO 7730 (2005), there are six primary factors that must be addressed when defining conditions for thermal comfort: metabolic rate, clothing insulation, air temperature, radiant temperature, air speed and humidity. Thermal comfort can be assessed through two primary metrics, i.e. PMV and PPD. The PMV predicts the mean response of building occupants based on the ASHRAE thermal sensation scale ranging from the value of −3 to +3, corresponding to cold and hot relative to optimum comfort condition. PMV is a function of four environmental variables, namely air temperature T_{air}, mean radiant temperature T_{rad}, air velocity v, and air humidity p_{air}, and also of the clothing insulation I_{cl} and the person's metabolic rate M. Thus, it can be written:

$$\text{PMV} = f\left(T_{air}, T_{rad}, v, p_{air}, I_{cl}, M\right) \qquad (10)$$

On the other hand, the PPD predicts the proportion of occupants dissatisfied with the specified thermal conditions. Based on experimental studies in which participants voted on their thermal sensation, an empirical relationship between PMV and PPD was developed as:

$$\text{PPD} = 100 - 95\exp\left(-0.3353PMV^4 - 0.2179PMV^2\right) \qquad (11)$$

In the present work, values of PMV and PPD have been considered as main parameters to evaluate indoor thermal comfort at defined positions, namely working desks and central point of the office room. The adopted values for the metabolic rate, clothing insulation and relative humidity are 1.2 met, 1.0 clo and 60%, respectively. In

addition, the local thermal discomfort caused by a vertical air temperature difference between head and ankles of the occupant and by the radiant temperature asymmetry has been assessed for the positions under study. According to ASHRAE (2013), allowable vertical air temperature difference between head and ankles is $\Delta T_{air} < 3°C$ and allowable radiant temperature asymmetry due to cool wall is $\Delta T_{rad} < 10°C$.

A finite volume CFD code implemented in ANSYS Fluent was employed for a 3D fluid flow and heat transfer analysis. The governing differential equations were solved by means of the control volume approach, which converts the governing equations to a set of algebraic discretized equations. Second-order discretization method was used for the pressure, momentum and energy terms, and the well-known SIMPLE (Semi-Implicit Method for Pressure-Linked Equation) was used to solve the pressure-velocity coupling. A 3D *TGrid* unstructured mesh composed of tetrahedral elements was generated by employing the Gambit software. The computational domain contains 2 799 219 tetrahedral cells. The mesh independence of the results was assured by performing preliminary computations with different meshes.

3. Experimental measurements and the model validation

The determination of the temperature in the 3D measurement grid was carried out with an innovative patented system (Guidorzi 2017) which measures the distance of the temperature sensor (a thermocouple) from some known points, similar to the principle of the GPS. Analytically, the problem is addressed by solving a system of 4 equations with 4 unknowns through a specific trilateration algorithm, which include the four distances of the target from four known points and the three spatial coordinates associated to four known points (Thompson 1998). The 4 distances are measured by means of acoustic waves: 4 different MLS (Maximum Length Sequence) signals orthogonal to each other are emitted simultaneously by 4 small loudspeakers placed on a grid, all in a known position (Rife and Vanderkooy 1989), as demonstrated in **Figures 3a** and **4**. The microphone, fixed very close to the thermocouple as shown in **Figure 3c**, samples the 4 MLS signals, which, despite being emitted at the same time, can be discriminated and through the Fast-Hadamard Transform algorithm are converted into 4 distinct impulse responses, as shown in **Figure 5b**. From the peak of these impulse responses, the flight time of the sound from the respective loudspeaker to the single microphone is calculated. Knowing the speed of sound, corrected according to the average air temperature for more accuracy, the 4 distances from the microphone to the 4 known points (loudspeakers) are obtained and with the algorithm described above, the position in the 3D space of the microphone and thermocouple is found (Guidorzi 2017). The idea of the position detection system was born from the need to correctly position microphones during measurements on road noise barriers (Garai and Guidorzi 2015). The temperature from the thermocouple is detected by an Arduino system, as shown in **Figure 3b**, interfaced directly with the software for measuring the position on the computer, illustrated in **Figure 5a**. The temperature measurement sub-system allows a resolution of 0.25 degrees.

The CFD model was validated by means of experimental temperature measurement, as explained above. In order to evaluate the accuracy of numerical model, 32 positions randomly spread inside the room were considered (**Figure 4**). For each position, the value of temperature measured by experimental test was compared with that obtained by CFD results. The average reported error of temperature evaluation was 3.6% with reference to experimental data, with a range of variation from 0.1 to 9.5%. This can be considered a satisfying model validation.

In addition, values of the air velocity were measured and compared to the numerical results. Since the air velocity inside the room is too low, in particular for the positions far from the fan coil, 5 different points near the fan coil were selected and measured with an air velocity meter (anemometer), with accuracy ±0.015 m/s. The considered points were selected at distance between 0.6–1.1 meter
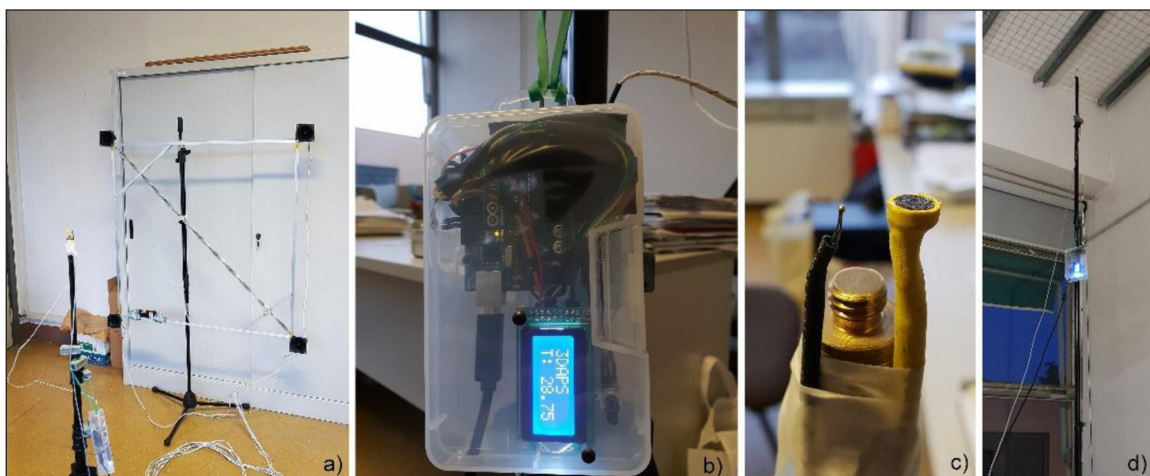

Figure 3: Measurement system: **a)** loudspeaker grid and microphone/thermocouple; **b)** detail of the Arduino system for reading the temperature from the thermocouple, interfaced with the measurement software on the computer; **c)** detail of the microphone and thermocouple; **d)** example of measurement in a high position.
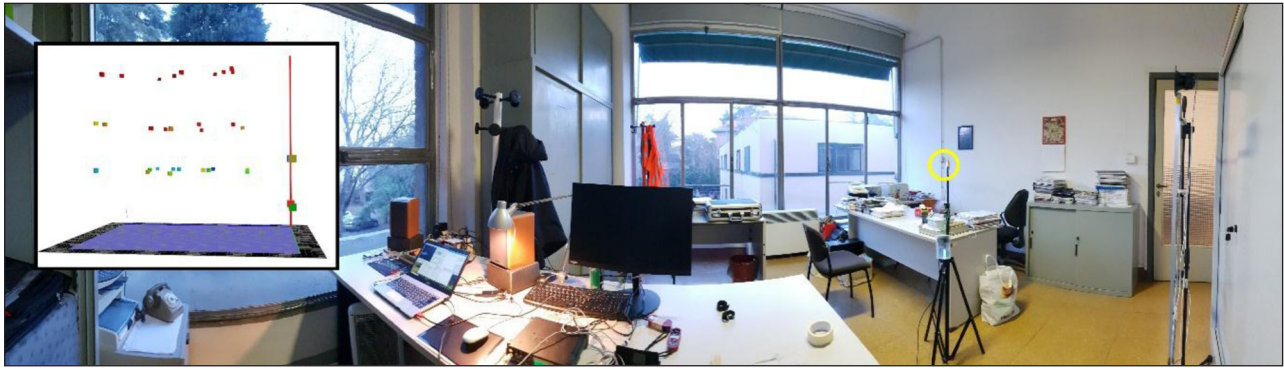
Figure 4: Panoramic view of the room being measured; the measured points are visible in 3D inside the box.
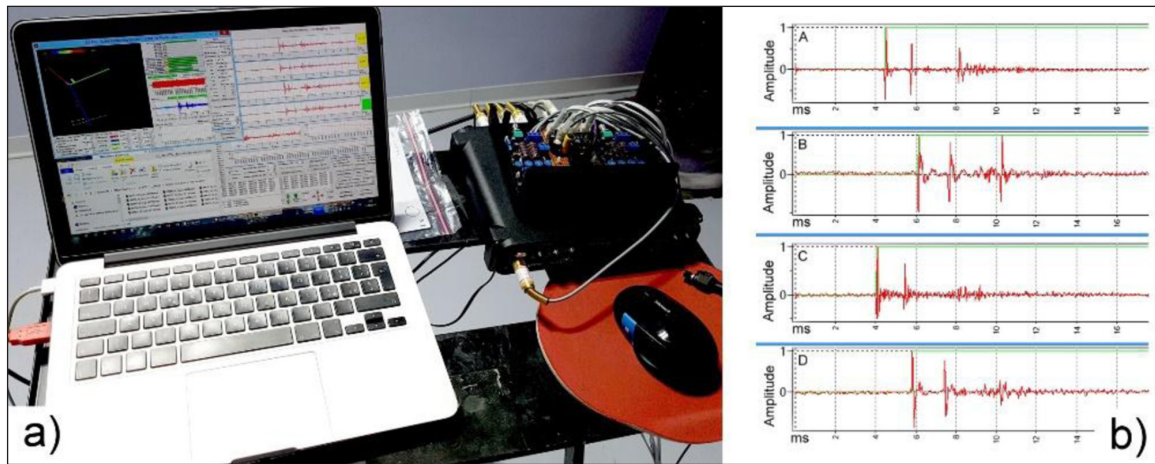

Figure 5: a) Measurement system: software and hardware components (microphone preamplifier, loudspeakers power amplifiers, multi-channel soundcard); **b)** example measurement of the four impulse responses sampled by the microphone.

from the fan coil with height between 1–2 meter from the floor. **Table 1** compares values of the air velocity yielded by experiments and those obtained by numerical simulations. The mean square deviation of numerical results from experimental data is 0.038 m/s. The comparison shows a good agreement between experimental and numerical results.

4. Results and discussion

The distribution of the air temperature and velocity, obtained by numerical simulations, allows to understand the thermal behaviour of the office room during a typical winter day whilst the heating system works in a stationary condition at fixed velocity and inlet temperature of the fan coil, as usual in centralised plants without local control systems.

Figures 6 and **7** illustrate air temperature and velocity distribution in a vertical section of the room for two different periods of a day, namely at morning and afternoon. The figures demonstrate clearly the effect of mixed convection inside the office room. In **Figure 6**, the vertical air stratification is evident from floor level to ceiling which is limited to an acceptable range of temperatures thanks to fan coil outlet air direction at 45°, while worst conditions would have occurred in case of vertical outlet air. The figure shows that the temperature distribution in the lower half of the vertical plane is

Table 1: A comparison for the values of air velocity: experimental vs. numerical.

Position	distance from fan coil (m)	distance from floor (m)	v_{exp} (m/s)	v_{num} (m/s)
a	0.6	1.0	0.05	0.06
b	0.6	1.5	0.11	0.12
c	0.6	2.0	0.52	0.43
d	1.1	1.5	0.01	0.02
e	1.1	2.0	0.02	0.04

more uniform in the afternoon, due to solar irradiation effect.

Figure 7 demonstrates that in vicinity of the outlet vent of fan coil, the forced condition due to air velocity is prevalent and streamlines follow the outlet direction; in the upper half of the room, the air velocity reduces to some extent and the chimney effect is more evident together with the induction effect which creates vortices and increases the air velocity on top of the room. This effect is more evident in the morning when the difference between the mean room temperature and the fan coil outlet air temperature is higher than afternoon.

The horizontal temperature map illustrated in **Figure 8**, at the height 1.2 m above the floor, shows a
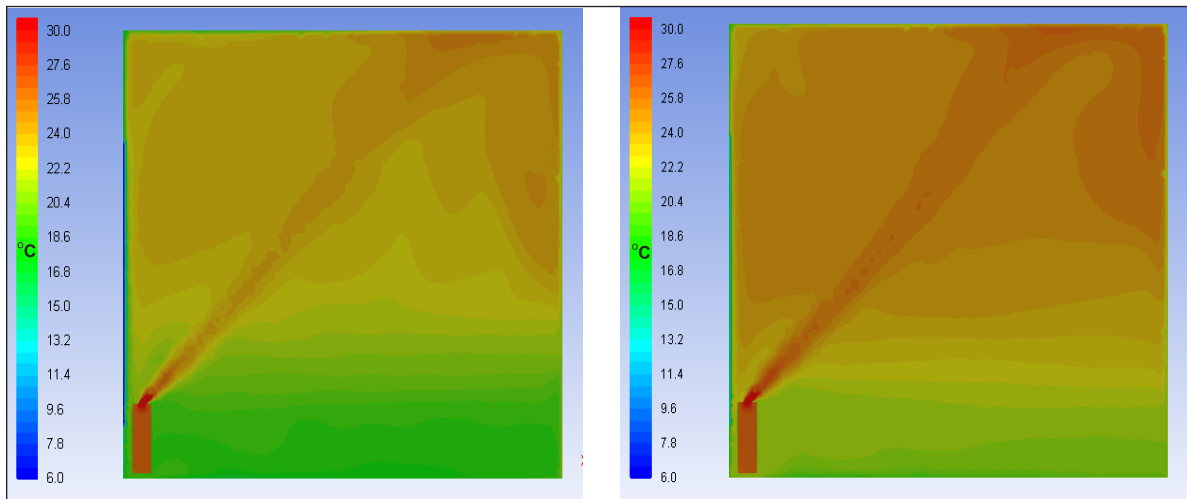
Figure 6: Temperature distribution in a vertical plane in middle of the room, at 9:00 (left) and at 15:00 (right).
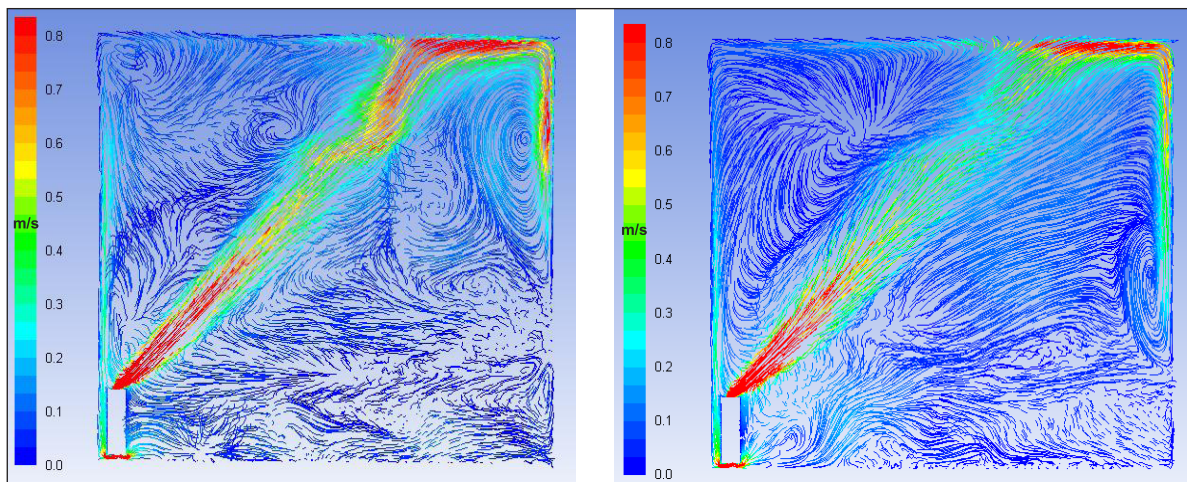

Figure 7: Velocity pathline in a vertical plane in middle of the room, at 9:00 (left) and at 15:00 (right).
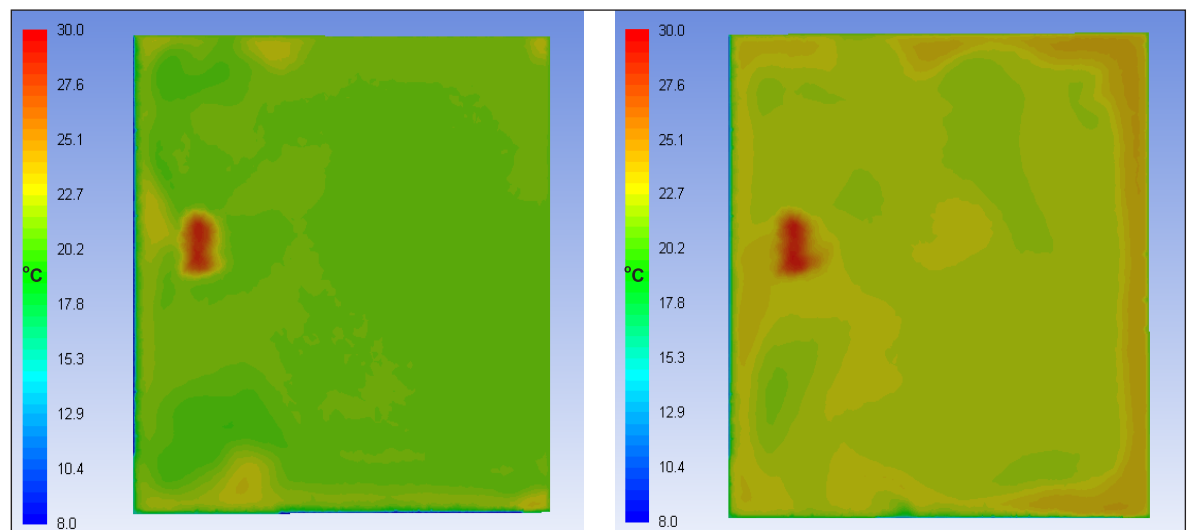

Figure 8: Temperature distribution in a horizontal plane at height 1.2 m, at 9:00 (left), and at 15:00 (right).

general uniform distribution inside the room, varying from 20 to 21°C at 9:00 and 22 to 23°C at 15:00, except for the zone in front of the fan coil with higher temperature. It can be noted that lateral positions of the fan coil (see also the values of position 3 in **Table 2**) assume the air temperature 0.5–1.2°C lower than central zone, due to reduced mixing effect.

The lack of temperature control (thermostat) in the office room causes that fan coil operates always at same conditions, and at fixed water temperature and fan speed

(unless manual variation of fan speed); for this reason, the internal temperature can undergo large variation during the day, as shown in the figures.

Even if the air temperature is within usual set point for offices buildings, actual comfort conditions are strongly influenced by radiation from internal surfaces. **Table 2** reports the results of operative temperature (T_{opr}), Predicted Mean Value (PMV) and related Predicted Percentage Dissatisfied (PPD) in 4 different hours of a day, for 5 considered positions. The table shows that due to large surface and low performance of windows, the radiant temperature reduces substantially T_{opr}, especially in the morning when the external temperature is lower. The results show that the comfort indexes at positions 1 and 3 are undesirable since these positions are located near the windows and have higher difference between the values of T_{air} and T_{rad}.

Table 2 shows that T_{opr}, in the morning (at 9:00), ranges from 17.5°C in position 1 to 19.3°C in position 5, with corresponding PMV of −0.68 and −0.32, respectively. It can be observed that in whole office room a general condition of "slightly cool" is prevalent. At other times of the day, the mean radiant temperature increases to some extent, compared with the morning. In addition, due to the solar radiation effect, the air temperature increases about 1°C, with maximum values

at 15:00, namely 22.5–23.0°C. For the whole day, PMV takes negative values for all working positions. However, the comfort criterion is satisfied for positions 2, 4 and 5. It can be concluded that a minimum distance of 2 m from windows is required in order to lower the radiating effect of the windows and consequently to have an acceptable thermal comfort condition.

In order to guarantee the indoor thermal comfort condition, it is necessary to analyse local discomfort parameters such as the effects of the vertical air temperature difference and radiant asymmetry inside the room. The corresponding results of the vertical air temperature difference and radiant asymmetry are reported in **Table 3**.

Vertical air temperature difference, ΔT_{air}, evaluated between head and ankles of a sitting person (0.1 to 1.1 m) is always below 3°C, as recommended by ISO 7730 in order to have PPD <5%. This difference takes into account only the effect of air flow due to the fan coil operation: in many real cases windows infiltrations and opening doors near colder zones causes higher ΔT_{air}.

Maximum horizontal radiant temperature asymmetry, $\Delta T_{rad, max}$, caused by cool windows, gives the highest values in position 1 for the whole day. In particular, this difference exceeds 10°C giving a PPD of almost 15% in morning ours (see value at 9:00). As reported in ISO 7730, PPD

Table 2: The values of the air, mean radiant and operative temperature, PMV, and PPD.

Position	9:00					Position	12:00				
	T_{air} (°C)	T_{rad} (°C)	T_{opr} (°C)	PMV	PPD		T_{air} (°C)	T_{rad} (°C)	T_{opr} (°C)	PMV	PPD
1	21.16	13.89	17.52	−0.68	14.83	1	22.08	16.47	19.28	−0.33	7.24
2	21.13	16.74	18.93	−0.42	8.76	2	22.06	17.78	19.92	−0.21	5.89
3	20.65	15.10	17.88	−0.64	13.52	3	21.85	16.43	19.14	−0.36	7.77
4	21.29	16.52	18.90	−0.42	8.76	4	21.83	17.58	19.70	−0.26	6.36
5	21.87	16.89	19.38	−0.32	7.07	5	22.48	17.88	20.18	−0.14	5.43
Position	15:00					Position	18:00				
	T_{air} (°C)	T_{rad} (°C)	T_{opr} (°C)	PMV	PPD		T_{air} (°C)	T_{rad} (°C)	T_{opr} (°C)	PMV	PPD
1	22.27	17.37	19.82	−0.25	6.28	1	21.70	15.87	18.79	−0.43	8.90
2	22.52	18.46	20.49	−0.08	5.15	2	21.66	17.42	19.54	−0.29	6.78
3	22.62	17.39	20.00	−0.30	6.85	3	21.21	16.07	18.64	−0.48	9.74
4	22.42	18.29	20.36	−0.11	5.27	4	21.84	17.20	19.52	−0.29	6.75
5	23.19	18.58	20.88	0.01	5.01	5	22.36	17.58	19.97	−0.19	5.73

Table 3: The values of vertical air temperature difference and radiant temperature asymmetry.

Position	9:00		12:00		15:00		18:00	
	ΔT_{air} (°C)	$\Delta T_{rad,max}$ (°C)	ΔT_{air} (°C)	$\Delta T_{rad,max}$ (°C)	ΔT_{air} (°C)	$\Delta T_{rad,max}$ (°C)	ΔT_{air} (°C)	$\Delta T_{rad,max}$ (°C)
1	2.44	10.16	2.13	7.58	2.26	6.34	2.41	8.86
2	2.61	7.02	2.51	5.29	2.52	4.33	2.59	6.01
3	2.39	6.22	2.08	5.03	2.18	4.25	2.28	5.49
4	2.52	8.26	2.20	6.47	1.80	5.42	2.81	7.28
5	2.73	5.83	2.37	4.59	2.82	3.76	2.81	5.02

increases rapidly with ΔT_{rad} leading to higher discomfort condition in winter season.

5. Conclusions

A 3D Computational Fluid Dynamic (CFD) code has been employed to evaluate thermo-hydraulic comportment inside a historic university office, built with thick masonry walls and large glass windows using fan coil as an air conditioning system. By means of finite volume method, turbulent air flow and local heat transfer characteristics of the room have been analysed for a typical winter day and thermal comfort indexes for working places inside the office have been determined. An innovative experimental set-up based on acoustic sources has been used to validate the numerical model and to obtain required initial and boundary conditions.

The obtained results show that even when the air temperature is quite uniform inside the room, the presence of low insulated envelope such as large glass windows leads to lower radiant temperature and as a consequence, to have higher possibility of local discomfort. Furthermore, the lack of local control system (thermostat) causes large variation in comfort conditions during working day which demands higher energy consumption. The results indicate that internal layout of working desks should be rearranged in the way that enough space between the working desks and the windows be taken into account in order to have a local comfort condition.

It can be concluded that CFD is an important tool allowing evaluation of local comfort sensation and optimization of thermal comfort in a specific workstation. Moreover, it could be used to evaluate innovative approaches to improve comfort indexes. The possibility of thermal comfort optimization together with local control of heating system leads to significant energy saving results. A potential direction for the future research is to assess the effect of using double-glazed windows on indoor comfort indexes for the similar historic buildings having large windows to wall surface ratio and a centralized heating system.

Competing Interests

The authors have no competing interests to declare.

References

ASHRAE. 2009. Handbook Fundamentals – IP Edition. Atlanta, USA.

ASHRAE. 2013. ASHRAE STANDARD 55. Thermal Environmental Conditions for Human Occupancy. Atlanta, USA.

Awwad, A, Mohamed, M and **Fatouh, M.** 2017. Optimal design of a louver face ceiling diffuser using CFD to improve occupant's thermal comfort. *Journal of Building Engineering*, 11: 134–157. DOI: https://doi.org/10.1016/j.jobe.2017.04.009

Buratti, C, Palladino, D and **Moretti, E.** 2017. Prediction of indoor conditions and thermal comfort using CFD simulations: A case study based on experimental data. *Energy Procedia*, 126: 115–122. DOI: https://doi.org/10.1016/j.egypro.2017.08.130

Catalina, T, Virgone, J and **Kuznik, F.** 2009. Evaluation of thermal comfort using combined CFD and experimentation study in a test room equipped with a cooling ceiling. *Building Environ*, 44: 1740–1750. DOI: https://doi.org/10.1016/j.buildenv.2008.11.015

Chen, Q. 1999. Comparison of different k-e models for indoor airflow computations. *Numerical Heat Transfer*, 28: 4391–4409. Part B: Fundamentals.

Cheong, KH, Teo, YH, Koh, JM, Acharya, UR and **Yu, SCM.** 2020. A simulation-aided approach in improving thermal-visual comfort and power efficiency in buildings. *Journal of Building Engineering*, 27: 100936. DOI: https://doi.org/10.1016/j.jobe.2019.100936

Cheong, KWD, Djunaedy, E, Chua, YL, Tham, KW, Sekhar, SC, Wong, NH and **Ullah, MB.** 2003. Thermal comfort study of an air-conditioned lecture theatre in the tropics. *Building Environ*, 38(1): 63–73. DOI: https://doi.org/10.1016/S0360-1323(02)00020-3

Choudhury, D. 1993. Introduction to the Renormalization Group Method and Turbulence Modelling. *Technical Memorandum TM-107*. Lebanon, NH: Fluent Inc.

Fanger, PO. 1970. Thermal comfort, analysis and application in environmental engineering. Copenhagen, Denmark: Danish Technical Press.

Fotopoulou, A, Semprini, G, Cattani, E, Schihin, Y, Weyer, J, Gulli, R and **Ferrante, A.** 2018. Deep renovation in existing residential buildings through façade additions: A case study in a typical residential building of the 70s. *Energy and Buildings*, 166: 258–270. DOI: https://doi.org/10.1016/j.enbuild.2018.01.056

Garai, M and **Guidorzi, P.** 2015. Sound reflection measurements on noise barriers in critical conditions. *Building and Environment*, 94(2): 752–63. DOI: https://doi.org/10.1016/j.buildenv.2015.06.023

Guidorzi, P. 2017. Patent Application nr. 102017000066160, filed on 14/06/2017 by the University of Bologna, inventor: Paolo Guidorzi.

Hajdukiewicz, M, Geron, M and **Keane, MM.** 2013. Calibrated CFD simulation to evaluate thermal comfort in a highly glazed naturally ventilated room. *Building and Environment*, 70: 73–89. DOI: https://doi.org/10.1016/j.buildenv.2013.08.020

ISO 7730. 2005. Moderate thermal environment – Determination of the PMV and PPD indices and specification of the conditions for thermal comfort.

Italia Dati Climatici Gianni De Giorgio. https://energyplus.net/sites/all/modules/custom/weather/weather_files/italia_dati_climatici_g_de_giorgio.pdf.

Jahanbin, A and **Zanchini, E.** 2016. Effects of position and temperature-gradient direction on the performance of a thin plane radiator. *Applied Thermal Engineering*, 105: 467–473. DOI: https://doi.org/10.1016/j.applthermaleng.2016.03.018

Maivel, M, Konzelmann, M and **Kurnitski, J.** 2015. Energy performance of radiators with parallel and serial connected panels. *Energy and Buildings*,

86: 745–753. DOI: https://doi.org/10.1016/j.enbuild.2014.10.007

Maykot, JK, Rupp, RF and **Ghisi, E.** 2018. A field study about gender and thermal comfort temperatures in office buildings. *Energy and Buildings*, 178: 254–264. DOI: https://doi.org/10.1016/j.enbuild.2018.08.033

Nada, SA, El-Batsh, HM, Elattar, HF and **Ali, NM.** 2016. CFD investigation of airflow pattern, temperature distribution and thermal comfort of UFAD system for theater buildings applications. *Journal of Building Engineering*, 6: 274–300. DOI: https://doi.org/10.1016/j.jobe.2016.04.008

Nicol, F, Humphreys, M and **Roaf, S.** 2015. Adaptive Thermal comfort: foundations and analysis. NewYork, USA: Routledge. DOI: https://doi.org/10.4324/9781315765815

Papakonstantinou, KA, Kiranoudis, CT and **Markatos, NC.** 2000. Computational analysis of thermal comfort: the case of the archaeological museum of Athens. *Appl Math Model*, 24(7): 477–494. DOI: https://doi.org/10.1016/S0307-904X(99)00049-9

Putra, JCP. 2017. A study of thermal comfort and occupant satisfaction in office room. *Procedia Engineering*, 170: 240–247. DOI: https://doi.org/10.1016/j.proeng.2017.03.057

Raznjevic, K. 1976. Handbook of Thermodynamic Tables & Charts. McGraw-Hill.

Rife, DD and **Vanderkooy, J.** 1989. Transfer-function measurement with maximum-length sequences. *J. Audio Eng. Soc.*, 37(6): 419–444.

Rupp, RF, Vasquez, NG and **Lamberts, R.** 2015. A review of human thermal comfort in the built environment. *Energy and Buidlings*, 105: 178–205. DOI: https://doi.org/10.1016/j.enbuild.2015.07.047

Semprini, G, Marinosci, C, Ferrante, A, Predari, G, Mochi, G, Garai, M and **Gulli, R.** 2016. Energy management in public institutional and educational buildings: the case of the school of engineering and architecture in Bologna. *Energy and Buildings*, 126: 365–374. DOI: https://doi.org/10.1016/j.enbuild.2016.05.009

Sevilgen, G and **Kilic, M.** 2011. Numerical analysis of air flow, heat transfer, moisture transport and thermal comfort in a room heated by two-panel radiators. *Energy and Buildings*, 43: 137–146. DOI: https://doi.org/10.1016/j.enbuild.2010.08.034

Shahzad, S, Calautit, JK, Aquino, AA, Nasir, DSNM and **Hughes, BR.** 2017. A user-controlled thermal chair for an open plan workplace: CFD and field studies of thermal comfort performance. *Applied Energy*, 207: 283–293. DOI: https://doi.org/10.1016/j.apenergy.2017.05.118

Shan, X, Xu, W, Lee, Y and **Lu, W.** 2019. Evaluation of thermal environment by coupling CFD analysis and wireless sensor measurements of a full-scale room with cooling system. *Sustainable Cities and Society*, 45: 395–405. DOI: https://doi.org/10.1016/j.scs.2018.12.011

Siegel, R and **Howell, JR.** 1992. Thermal radiation heat transfer. Washington, DC: Taylor & Francis.

Sontag, RE, Borgnakke, C and **Van Wylen, GJ.** 2003. Fundamentals of Thermodynamics. Sixth ed. John Wiley & Sons.

Stamou, A and **Katsiris, I.** 2006. Verification and application of a CFD model for the evaluation of thermal comfort in office spaces. *Building Environ*, 41: 1171–181. DOI: https://doi.org/10.1016/j.buildenv.2005.06.029

Stamou, AI, Katsiris, I and **Schaelin, A.** 2008. Evaluation of thermal comfort in Galatsi Arena of the Olympics Athens 2004 using a CFD model. *Appl Therm Eng.*, 28(10): 1206–1215. DOI: https://doi.org/10.1016/j.applthermaleng.2007.07.020

The Directive 2010/31/EU of the European Parliament and of the Council of 19 May 2010 on the Energy Performance of Buildings (EPDB).

Thompson, RB. 1998. Global Positioning System: The Mathematics of GPS Receivers. *Mathematics Magazine*, 71(4): 260–269. DOI: https://doi.org/10.1080/0025570X.1998.11996650

Tsilingiris, PT. 2008. Thermophysical and transport properties of humid air at temperature range between 0 and 100°C. *Energy Conversion and Management*, 49: 1098–1110. DOI: https://doi.org/10.1016/j.enconman.2007.09.015

Versteeg, HK and **Malalasekera, W.** 1995. An Introduction to Computational Fluid Dynamic. Longman.

Yakhot, V, Orszag, SA, Thangam, S, Gatski, TB and **Speziale, CG.** 1992. Development of turbulence models for shear flows by a double expansion technique. *Physics of Fluids A*, 4: 1510–1520. DOI: https://doi.org/10.1063/1.858424